American Mineralogist, Volume 88, pages 1731–1740, 2003

On the formation of peridotite-derived Os-rich PGE alloys

FRANK E. BRENKER,[1,*] ANDERS MEIBOM,[2] AND ROBERT FREI[3]

[1]Institut für Mineralogie und Geochemie, Universität zu Köln, Zülpicher Str. 49b, 50674 Köln, Germany
[2]Geological & Environmental Sciences, 320 Lomita Mall, Stanford University, California 94305-2115, U.S.A.
[3]Geological Institute, University of Copenhagen, Øster Voldgade 10, DK-1350 Copenhagen, Denmark

ABSTRACT

Osmium-rich Pt group element (PGE) alloys occur worldwide in association with chromite in ultramafic (peridotite) complexes. It has been suggested that these Os-rich alloys formed under extreme *P-T* conditions in the lowermost mantle, before the metallic core of the Earth formed, or later, in the outer core, and have been transported to the upper mantle as xenoliths in deep-rooted mantle plumes.

Our investigation of syn- and pregenetic inclusions (including silicate and chromite) found in Os-rich alloys from peridotites in northern California and southwest Oregon yield no evidence that these alloys formed under extreme *P-T* conditions. Instead these inclusions point to a hydrous magmatic origin in the shallow upper mantle, most likely in an arc-environment. Indeed, the common occurrence of Os-rich PGE alloys as primary inclusions in massive (commonly podiform), chromite deposits and, conversely, the occurrence of chromite, olivine, pyroxene, laurite, and siliceous (boninitic) melt inclusions in Os-rich PGE alloys suggest a common origin for all these minerals.

Integrating our observations with recent experimental work and with observed field relations, we find support for a model in which massive chromite deposits, olivine, laurite, and Os-rich PGE alloys form in a single magmatic process. In an arc-environment, H_2O-rich fluids and siliceous melts (e.g., boninites) are produced in the mantle wedge above the descending and dehydrating plate. Large differences in interfacial energy between the precipitated chromite and PGE alloys, and the hydrous fluid(s) and siliceous melt(s), cause a strong concentration of chromite and PGE alloys in the hydrous fluid(s). This general scenario is capable of simultaneously explaining all key observations, including: (1) the formation of massive chromite deposits; (2) nodular chromite textures; (3) Os-rich PGE alloys, laurite, olivine, and pyroxene as common inclusions in massive chromite; (4) inclusions of chromite, olivine, pyroxene, and hydrated siliceous inclusions (the current study) in the Os-rich PGE alloys; and (5) a similar range of variation in $^{187}Os/^{188}Os$ ratios among Os-rich PGE alloys and massive chromite deposits from individual ultramafic bodies world-wide.

INTRODUCTION

Material from the deep regions of the Earth's mantle is extremely scarce. This scarcity limits our efforts to explore in detail the chemistry and mineralogy of mantle phases below the transition zone. It has been argued that certain inclusions in diamonds (e.g., Harte and Harris 1994; Stachel et al. 2000a, 2000b; Brenker et al. 2002) and probably also a suite of small xenoliths from Malaita (Collerson et al. 2001) may indeed originate in the transition zone or from the lower mantle. These two occurrences might be the only known examples of minerals that have preserved their chemical (and perhaps structural) information during ascent from the deep mantle. However, already decades ago it was proposed that rocks called "josephinite" from the Josephine ophiolite in southwest Oregon and northern California, which contain a high proportion of Ni-rich FeNi metal (awaurite), might have originated from the outer core of the Earth or the core-mantle boundary region and was transported up to the surface of the Earth as xenoliths in deep-rooted mantle plumes (Bird and Weathers 1975, 1979; Bird et al. 1979). This idea was abandoned by the vast majority of researchers as it became clear that Ni-rich FeNi metal is easily formed under the reducing conditions prevailing during serpentinization of ophiolites (e.g., Chamberlain et al. 1965; Dick 1974; Eckstrand 1975; Dick and Gillete 1976; Sleep et al. 2003). A case also was made that mantle-derived Os- and Ir-rich PGE alloys (osmiridium and iridosmine), occurring in chromite-rich placers in southwest Oregon and northern California, but not otherwise related to josephinite, either are primordial materials that have survived since the formation of the Earth, or formed as the result of melting in one of three alternative scenarios: (1) in the lower mantle in the early Earth when mantle temperatures were higher than at present; (2) in the mantle at depths greater than 2900 km before that region was occupied by the core; or (3) in the outer core (Bird and Bassett 1980). These inferences were based on petrologic observations of complex PGE alloy intergrowths suggesting that these alloys crystallized from a melt, a hypothesized phase change argued to reflect pressure release as the alloys were transported to the upper mantle, and extremely high estimated melting temperatures (>3000 °C at deep mantle pressures) inferred by ex-

* E-mail: brenker@min.uni-koeln.de

0003-004X/03/1112–1731$05.00

trapolating binary phase diagrams (Os-Ir, Os-Ru, and Ir-Ru) to an assumed bulk composition of the initial melt combined with a pressure correction corresponding to lower mantle/outer core conditions (Bird and Bassett 1980). Scenarios 1 and 2 imply that the alloys formed early in the evolution of the Earth. All three scenarios require that the Os-rich PGE alloys subsequently were transported upward in the convecting mantle, e.g., by deep-rooted mantle plumes, and incorporated into depleted mantle lithosphere, now exposed as obducted ophiolites or peridotite bodies (Bird and Bassett 1980).

Osmium-rich PGE alloys occur world wide in association with peridotites as crystals enclosed in massive, podiform chromite (e.g., Stockman and Hlava 1984; Talkington et al. 1984; Melcher et al. 1997; Bai et al. 2000) or as detrital grains in chromite-rich placers produced by mechanical erosion of peridotite outcrops (Cabri et al. 1996). Most studies of these Os-rich PGE alloys have concluded that they formed by precipitation during the earliest stages of magma chamber crystallization in the lithospheric upper mantle (Stockman and Hlava 1984; Barnes et al. 1985; Tornroos and Vuorelainen 1987; Auge and Johan 1988; Hagen et al. 1990; Johan et al. 1990; McElduff and Stumpfl 1990; Nilsson 1990; Peck and Keays 1990; Peck et al. 1992; Fleet and Stone 1991; Leblanc 1991; Slansky et al. 1991; Cabri et al. 1996; Nakagawa and Franco 1997; Amossé et al. 2000; Brenan and Andrews 2001; Malitch and Thalhammer 2002; Ballhaus 1998; Matveev and Ballhaus 2002). Evidence for a magmatic origin of these peridotite-derived Os-rich PGE alloys comes from their association with podiform chromite and the common observation of inclusions with typical upper mantle mineralogy and chemistry, including chromite, olivine, pyroxene, and sulfides; notably laurite, but also chalcopyrite, bornite, and pentlandite (Hagen et al. 1990; Slansky et al. 1991; Cabri et al. 1996; Malitch and Thalhammer 2002; Malitch et al. 2002; Peck et al. 1992). Furthermore, well-defined exsolution patterns are observed in the PGE alloys, which can only form under high (i.e., mantle) temperatures.

Experimental and theoretical studies offer constraints on the temperature as well as the O and S fugacities during precipitation of these Os-rich PGE alloys and PGE-rich sulfides from silicate melts under upper mantle conditions (Stockman and Hlava 1984; Peck and Keays 1990; Peck et al. 1992; Nakagawa and Franco 1997; Rehkämper et al. 1999; Amossé et al. 2000; Brenan and Andrews 2001; Ballhaus 1995, 1998; Matveev and Ballhaus 2002). However, because of their intimate association with massive chromite deposits, any viable model for the formation of Os-rich PGE alloys will also have to address the formation of the chromite, including the question of how Cr is being concentrated from levels of 300–500 ppm in primitive mantle melts (Talkington et al. 1984; Matveev and Ballhaus 2002) to more than 50 wt% in massive chromite deposits. Preferentially, such a genetic model should also be able to explain the characteristic nodular textures of some undeformed chromitite deposits, as well as the presence of the different types of inclusions observed in the massive chromite and in the associated Os-rich PGE alloys.

Here we present a study of several syn- and pregenetic inclusions of chromite and silicates found in Os-rich PGE alloys collected from the Port Orford black sand (chromite-rich) placer deposits. We have examined these inclusions with a variety of analytical techniques in an attempt to further establish their environment of formation. We discuss our results in light of the various models proposed for the formation of the Os-rich PGE alloys and recent models for formation of podiform chromite.

Samples and analytical procedures

The samples studied here are millimeter-sized iridosmine and osmiridium grains collected from the black sand placer deposits near Port Orford, on the Pacific coast of Oregon (Bird and Bassett 1980; Bird et al. 1999; Meibom and Frei 2002; Meibom et al. 2002). These grains are derived from peridotite-bearing ophiolites in the Klamath and Siskiyou Mountains in northern California and southwestern Oregon, where they are known to occur in association with podiform chromite deposits (Stockman and Hlava 1984). Iridosmine is an Os-rich PGE alloy, which typically has a chemical composition in the range 55–90 wt% Os, 20–45 wt% Ir, and 0–10 wt% Ru. Osmiridium has 20–40 wt% Os, 80–55 wt% Ir, and 0–10 wt% Ru (Harris and Cabri 1973). Recently, the nomenclature of PGE alloys was modified and Os-rich (iridosmine) alloys are now simply referred to as osmium, and Ir-rich (osmiridium) alloys are referred to as "iridium" (Harris and Cabri 1991). The grains from Port Orford most likely were transported to the Pacific coast via one of several rivers that drain several peridotite bodies in southwest Oregon, including the Rogue River, Sixes River, and Elk River. The largest of these peridotite bodies is the Josephine ophiolite, which covers an area of more than 800 km^2. The Josephine ophiolite consists mainly of harzburgite overlain by scarce cumulate ultramafics, gabbro, diorite, sheeted dikes, and pillow lavas (Harper 1984). The harzburgitic peridotite section contains numerous massive, tectonized chromite deposits (Ramp 1961; Stockman and Hlava 1984). The lavas and dikes are chemically distinct from mid-ocean-ridge-basalt (MORB) but have affinities to island-arc, supra-subduction magmatism (Harper 1984). The Josephine ophiolite, along with a large fraction of ophiolites in this region, formed at one or more back-arc spreading centers that developed behind the magmatic arc complexes along the north Pacific rim, i.e., in a supra-subduction setting (Harper 1984; Harper et al. 1990; Coleman 2000).

We have surveyed more than 100 iridosmine and osmiridium grains collected in placer deposits near Port Orford. Samples were made available from the Cornell University mineral collection (labeled Port Orford Oregon 22-8) by J.M. Bird, and from the Yale Peabody Museum (labeled YPM MIN.1.182) by E. Faller. These grains were mounted in epoxy and polished down to a 1 micrometer finish using diamond suspensions. The epoxy mounts were studied with a reflected light optical microscope to search for non-metal inclusions. Inclusions were subsequently imaged in back-scattered electron mode on a JEOL JSM-5600LV electron microscope at the Stanford University.

The composition of the host metal grains were analyzed on a Cameca SX 50 at the Stanford University electron microprobe utilizing the $L\alpha$ lines for Os, Ir, Ru, Pt, and Re. Analytical conditions included an accelerating voltage of 25 kV, a beam current of ~30 nA, and a spot size of ~2 micrometer on the sample. Pure metals were used as standards. A correction was made for the Os $L\beta$ interference on the Re$L\alpha$ peak.

Non-metal inclusions were analyzed with a JEOL 8900 microprobe at the University of Cologne. Analytical conditions were 20 kV acceleration voltage and an ~2 mA beam current. Natural as well as synthetic silicate standards were used for calibration.

Subsequently, three inclusions (two silicate and one chromite) were removed from their host PGE alloy and crushed between two glass slides to produce small fragments transparent to high-energy electrons and therefore suitable for TEM work. TEM analyses were performed on a Philips CM12 transmission electron microscope with an acceleration voltage of 120 kV at the Technical University Darmstadt. Analytical TEM work involved selective area electron diffraction (SAED) and energy dispersive X-ray analysis (EDX) techniques. Chemical compositions were corrected using experimental determined *k*-factors applying the method of van Capellen and Doukhan (1994). Dark-field imaging as well as higher resolution lattice fringe electron micrographs were used to study structural details and to test for features related to phase transformations, such as twins or antiphase domains.

Results

Evidence for a negative crystal shape in host phases is often used to argue for syn-genetic growth of an inclusion. For example, this diagnostic feature is frequently used to distin-

guish between the pre-, syn-, and post-genetic origins of inclusions in diamond (e.g., Stachel et al. 2000a).

In the present study, we focus mainly on three of the investigated PGE grains (Table 1) in which we observed inclusions of chromite and silicates. In one case, we found evidence for several syn-genetic inclusions in an Os-rich PGE alloy. These inclusions consist of enstatite and glassy material and show typical pseudo-euhedral grain shapes (Fig. 1). Typically, the facets of all inclusions within the same host alloy are aligned exactly parallel (Fig. 1). Osmium- and Ir-rich PGE alloys crystallize either in the hcp (Os-rich, hexagonal closest packed) or in fcc (Ir-rich, face-centered cubic) structure. This is consistent with the shape of the inclusions, which indicate hexagonal or cubic symmetries.

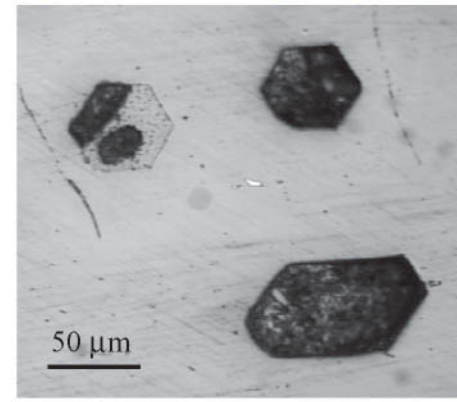

FIGURE 1. Reflected-light image of trapped melt inclusions in Os-rich PGE alloys (white). The facets of three syngenetic inclusions are aligned exactly parallel. Only the upper left inclusion is still filled. The other two inclusions were likely lost during the preparation process. The pseudo-euhedral shape suggests a negative crystal within the hexagonal or cubic symmetry of the host PGE alloy.

Silicate inclusions

Enstatite is the primary principal in these syngenetic inclusions, which are characterized by a large number of voids (Fig. 2a), suggestive of a high fluid content of the trapped melt. The low total (<98 wt%) of each measurement is most likely due to a high water content (Table 2). A complex intergrowth of at least two different phases can be recognized using back-scattered electron (BSE) imaging (Figs. 2a and 2b). The microstructure shows a clear relation to the shape of the inclusions (Fig. 2). The orientation of the phases is always perpendicular to the rim of the inclusion (Fig. 2a). In another inclusion (Fig. 2b), it can be seen that phases closer to the rim are smaller and their size increases toward the inner part of the inclusion. Both features indicate that the microstructure-forming process, i.e., crystallization from a melt, occurred after trapping within the PGE alloy. Due to the small grain size (less than 2 µm), the resolution of the electron microprobe was not adequate to identify these mineral phases based on their composition alone (see Table 2). For this reason, two syn-genetic inclusions were prepared for TEM investigation.

The only crystalline mineral phase found was enstatite (Table 3). The majority of the enstatite belong to space group *Pbca* (ortho-enstatite). However, a minor amount of clino-enstatite lamellae belonging to the $P2_1/c$ space group occurs in all ortho-enstatite crystals. Typically, the lamellae occur as sets containing an even number. In some cases we found partial dislocations at the tip of the clino-enstatite, which connect the lamellae with the ortho-enstatite host (Fig. 3). The second phase found in the silicate inclusions is amorphous. The composition of this amorphous phase (Table 3) does not correspond to that of any known mineral. It seems likely that the amorphous material represents a quenched and, therefore, glassy phase.

The high porosity and compositional heterogeneity of these silicate inclusions make it difficult to estimate precisely the composition of the original, trapped melt. However, we attempt to infer the bulk composition of the trapped melt from measurement of a very fine-grained inclusions that did not display larger crystals (measurement P5; Table 2). We have also calculated an average composition based on all measured data points (Table 2), each of which might include measurements of either predominantly glass or orthopyroxene, respectively. The estimated composition of the melt has been compared with literature data on different melt compositions encountered in different tectonic settings in the mantle. Our best estimate, the mean of all measurements, for the composition of the trapped melt is very similar to boninitic melts (Table 2).

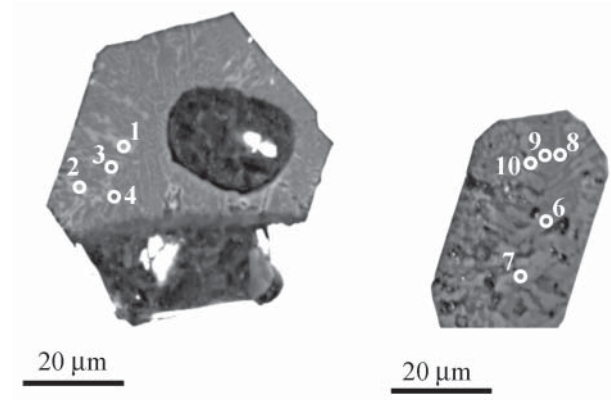

FIGURE 2. BSE images of trapped melt inclusions in Os-rich PGE alloy. (**a**) A bubble is located in the middle of the glass-orthopyroxene intergrowth. The arrangement of the darker and lighter gray arrays in the solid part of the inclusion suggest growth of at least one phase perpendicular to the rim of the inclusion. (**b**) A second inclusion with a high proportion of pore space. Again the phases seem to be aligned perpendicular to the rim of the inclusion. The size of the phases increase from rim to the center of the inclusion. Both features are indicative for growth in situ, after the melt was trapped in the PGE alloy. The numbers correspond to the compositions listed in Table 2.

TABLE 1. EPMA analyses of the chemical composition of the three host PGE alloys included in this study

Wt%	Grain 1	Grain 2	Grain 3
Os	32.1	56.5	45.8
Ir	63.8	36.8	39.6
Pt	1.9	1.8	0.74
Ru	1.2	4.3	14.1
Sum	99	99.4	100.24

For comparison, two boninitic melt compositions from the

TABLE 2. EPMA analyses of the chemical composition of the trapped melt

Sample	P1	P2	P3	P4	P5	P6	P7	P8	P9	P10	Mean	Boninite-Tr1	Boninite-Tr2
Na_2O	0.99	0.19	0.10	0.48	0.45	0.14	0.12	0.48	0.47	0.43	0.38	0.70	0.59
K_2O	0.02	0.00	0.02	0.00	0.03	0.06	0.04	0.24	0.31	0.14	0.08	0.10	0.08
SiO_2	47.44	49.02	48.31	55.01	55.00	52.98	51.51	56.43	55.42	53.93	52.50	52.40	52.00
FeO	3.94	5.53	6.05	3.83	3.98	2.11	2.57	1.74	1.61	1.80	3.31	8.40	9.14
NiO	0.22	0.23	0.21	0.00	0.00	0.28	0.08	0.16	0.06	0.14	0.14	n.d.	n.d.
TiO_2	0.06	0.05	0.11	0.08	0.09	0.07	0.08	0.08	0.09	0.10	0.08	0.30	0.23
Al_2O_3	14.74	11.95	11.04	14.53	14.68	9.25	6.36	14.02	15.16	10.42	12.21	11.70	11.81
MnO	0.06	0.07	0.10	0.12	0.11	0.15	0.17	0.12	0.10	0.15	0.12	n.d.	n.d.
CaO	7.14	11.98	13.50	8.90	9.21	3.95	18.93	8.05	8.37	12.95	10.30	10.70	9.82
MgO	9.84	16.52	17.71	15.30	14.95	27.72	14.17	12.56	9.15	15.38	15.33	15.80	16.33
Cr_2O_3	0.00	0.02	0.06	0.03	0.02	0.08	0.07	0.01	0.02	0.06	0.04	n.d.	n.d.
Sum	84.45	95.55	97.19	98.28	98.51	96.79	94.09	93.88	90.75	95.51	94.50	100.10	100.00
													2% H_2O
Na	0.16	0.03	0.01	0.06	0.06	0.02	0.02	0.07	0.07	0.06	0.06		
K	0.00	0.00	0.00	0.00	0.00	0.01	0.00	0.02	0.03	0.01	0.01		
Si	3.85	3.64	3.56	3.84	3.83	3.73	3.90	4.04	4.09	3.91	3.84		
Fe	0.27	0.34	0.37	0.22	0.23	0.12	0.16	0.10	0.10	0.11	0.20		
Ni	0.01	0.01	0.01	0.00	0.00	0.02	0.00	0.01	0.00	0.01	0.01		
Ti	0.00	0.00	0.01	0.00	0.00	0.00	0.00	0.00	0.00	0.01	0.00		
Al	1.41	1.04	0.96	1.19	1.21	0.77	0.57	1.18	1.32	0.89	1.05		
Mn	0.00	0.00	0.01	0.01	0.01	0.01	0.01	0.01	0.01	0.01	0.01		
Ca	0.62	0.95	1.07	0.67	0.69	0.30	1.54	0.62	0.66	1.01	0.81		
Mg	1.19	1.83	1.95	1.59	1.55	2.91	1.60	1.34	1.01	1.66	1.66		
Cr	0.00	0.00	0.00	0.00	0.00	0.00	0.00	0.00	0.00	0.00	0.00		
Sum	7.52	7.85	7.96	7.59	7.59	7.89	7.82	7.40	7.29	7.68	7.66		

Notes: Due to the small grain size the measurements (P1 to P10) always include orthopyroxene and residual melt, but in different amounts. Boninite-Tr1, Boninite-Tr2 are examples for boninitic melt compositions from the Troodos ophiolite (Sobolev and Chaussidon 1996).

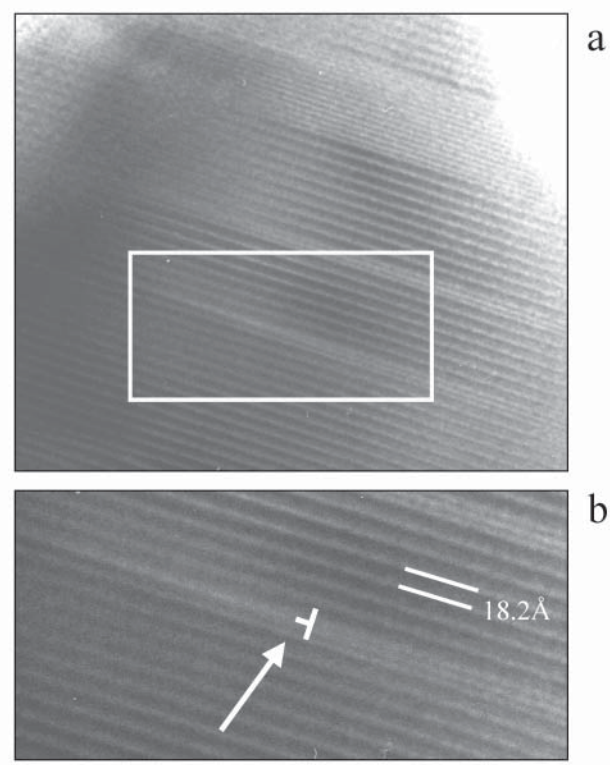

FIGURE 3. (**a**) Bright-field electron micrograph of (100) lattice fringes of orthoenstatite with lamellae of clinoenstatite. (**b**) Detail of (a) showing the shear mechanism, which produces two clinoenstatite lamellae from one orthoenstatite lamella. The required partial dislocation is indicated by symbol and arrow.

TABLE 3. EDX-TEM analyses of glass and enstatite

	Glass	Glass	Glass	Enstatite
		Mol% cation		
Na	3.22	2.77	2.55	1.30
Mg	0.69	1.06	0.00	49.60
Al	25.08	25.69	21.73	1.90
Si	59.98	59.76	66.29	44.30
K	0.59	0.51	0.72	0.20
Ca	9.68	9.74	8.27	1.80
Fe	0.80	0.47	0.44	0.80
Sum	100.04	100.00	100.00	99.90
		Wt% oxides		
Na_2O	1.77	1.52	1.39	0.81
MgO	0.49	0.76	0.00	40.26
Al_2O_3	22.68	23.25	19.44	1.95
SiO_2	63.92	63.74	69.89	53.60
K_2O	0.49	0.43	0.60	0.19
CaO	9.63	9.70	8.14	2.03
FeO	1.02	0.60	0.55	1.16
Sum	100.00	100.00	100.00	100.00

Note: Cations were normalized to 100%.

Troodos ophiolite are given in Table 2 (Sobolev and Chaussidon 1996). The similarity between the average composition of the inclusion and the boninitic melts is also consistent with the proposed high water content, as boninitic melts are the most H_2O-rich melts from the mantle of the earth (Falloon and Danyushevsky 2000; Sobolev and Chaussidon 1996).

Liquidus temperature of the silicate inclusions

Two approaches were taken to estimate the liquidus temperature of the silicate inclusions and, therefore, constrain the temperature at which the PGE alloy formed. In the first approach we calculated liquidus temperatures and crystallization sequences at pressures up to 2 GPa using the program MELTS release 1.1.0, 1999 (Ghiorso and Sack 1995; Asimow and Ghiorso 1998) (Table 5). In the second approach, we summarized experimental data on the formation of boninitic melts

TABLE 4. EDX-TEM analyses of chromite inclusion from PGE alloy

	PGE Cr1	PGE Cr2	PGE Cr3	PGE Cr4	c.r. TP	c.r. SR	l.m. 1-35	l.m. 4-4	l.m. 5-17a	l.m. 5-17b	l.m. 5-55
						wt% oxide					
FeO	**14.76**	**16.76**	**16.12**	**18.56**	**17.13**	**14.21**	**33.72**	**33.34**	**33.44**	**33.53**	**33.58**
MgO	14.00	6.83	8.71	5.79	13.03	14.09	10.54	10.76	10.60	10.72	10.68
Al_2O_3	12.23	6.35	7.85	5.93	7.96	7.51	5.32	5.38	5.25	5.37	5.31
Cr_2O_3	**59.01**	**70.05**	**67.32**	**69.72**	**60.97**	**63.83**	**35.79**	**36.33**	**35.45**	**36.34**	**36.23**
TiO_2	**<1.00**	**<1.00**	**<1.00**	**<1.00**	**0.35**	**0.2**	**10.79**	**10.86**	**11.12**	**10.73**	**10.65**
MnO	<1.00	<1.00	<1.00	<1.00	0.55	0.62	0.77	0.74	0.75	0.79	0.75
						Cation calculated for 4 oxygen atoms					
Fe	0.39	0.48	0.45	0.54	0.47	0.39	1.00	0.98	0.99	0.99	0.99
Mg	0.66	0.35	0.44	0.30	0.64	0.68	0.56	0.57	0.56	0.56	0.56
Mn	<0.01	<0.01	<0.01	<0.01	0.02	0.02	0.02	0.02	0.02	0.02	0.02
Al	0.46	0.26	0.31	0.24	0.31	0.29	0.22	0.22	0.22	0.22	0.22
Cr	1.48	1.91	1.80	1.92	1.59	1.65	1.00	1.01	1.00	1.01	1.01
Ti	<0.01	<0.01	<0.01	<0.01	0.01	0.01	0.29	0.29	0.30	0.29	0.28
Sum	3.00	3.00	3.00	3.00	3.04	3.04	3.09	3.09	3.09	3.09	3.08
Cr/(Cr + Al)	0.76	0.88	0.85	0.89	0.84	0.85	0.82	0.82	0.82	0.82	0.82
*P*max	4.5 GPa	5.8 GPa	5.4 GPa	6 GPa	5.3 GPa	5.4 GPa	–	–	–	–	–

Note: Cations were calculated for 4 O atoms. For comparison two chromite compositions from the port Orford ophiolite (country rocks = c.r.) (Stockman and Hlava 1984) and four from the unusual occurrence in association with typical lower mantle/transition zone phases in diamonds from the Juina area (lower mantle = l.m.) (Kaminsky et al. 2000) are given.

(Falloon and Danyushevsky 2000; Umino and Kushiro 1989; Van der Laan et al. 1989), and compared our calculations and extrapolations from the experimental data with the model of Matveev and Ballhaus (2002).

Calculations using MELTS. For our calculations, we used both the representative analysis P5 and the average composition of all measurements. Each measured point represents variable contents of residual melt plus orthopyroxene. The difference in calculated liquidus temperatures using different melt compositions is small, however, compared with the effects of pressure and water content. Assuming pressures of 0.2, 0.5, 1, 1.5, and 2 GPa, we obtained liquidus temperatures between 1390 and 1667 °C (Table 4). Linear extrapolation toward higher pressure shows an increase in the liquidus temperature of around 140 °C/GPa. Conversely, a high water content will decrease the calculated temperature substantially. Assuming 5 or 10 wt% H_2O, we calculated a liquidus temperature between 1270 (10 wt% H_2O, 0.2 GPa) and 1519 °C (5 wt% H_2O, 2 GPa). Because the pressure of formation and H_2O content of silicate melt inclusion are largely unconstrained, we can only estimate a minimum liquidus temperature of more than 1250 °C. The first mineral phase to crystallize from such a melt is either enstatite with low concentrations of Ca, Fe, and Al, which is in good agreement with our measurements (Table 3), or olivine. At very low pressures (<0.5 GPa) or high fluid contents, olivine will be the first phase to crystallize.

Experimental data. Large experimental data sets relevant to the formation of high-Ca boninites are available in the literature (Falloon and Danyushevsky 2000; Umino and Kushiro 1989; Van der Laan et al. 1989). In our second approach to estimate realistic liquidus temperatures of the trapped boninitic melt in the PGE alloy, we first summarized these data and then extrapolated these obtained values to the conditions proposed by Matveev and Ballhaus (2002).

The result of the experimental work shows some disagreement with regard to the formation temperature of high-Ca boninite magmas. Falloon and Danyushevsky (2000) reported temperatures of 1430–1480 °C at 1.5 GPa and 1–2 wt% H_2O for the petrogenesis of this rock type. They found that the liquidus temperature decreased with increasing H_2O-content. The liquidus depression was found to be (in °C): $74.403° (H_2O\ wt\%)^{0.352}$, corresponding to 95 and 167 °C for 2 and 10 wt% H_2O, respectively. In contrast Umino and Kushiro (1989) and Van der Laan et al. (1989) suggested temperatures between 1130 and 1260 °C in the pressure range of 0.3 to 1.8 GPa, and water contents ranging from 1 to 20 wt%.

Comparison of predicted conditions, calculation, and experimental data. Matveew and Ballhaus (2002) proposed that podiform chromites are formed close to the Moho at a pressure of 0.2 GPa and temperatures around 1250–1150 °C. The water content in their experiment was about 4 wt%. Boninitic melts can be considered an end-member melt composition in a supra-subduction setting as their formation requires the highest formation temperatures and high H_2O concentrations (Falloon and Danyushevsky 2000).

Under the same conditions, i.e., a high water content (> 4 wt% H_2O) in the trapped melt and low pressure (0.2 GPa), our calculated liquid temperatures range from 1270 to 1320 °C.

To compare the experimental data of Falloon and Danyushesky (2000), we must extrapolate their data to the same conditions. The effect of reducing the pressure from 1.5 to 0.2 GPa on the liquidus is estimated from comparison with our calculated values (Table 4) to be 100–120 °C. The extrapolated liquidus temperature at these conditions (0.2 GPa, 4 wt% H_2O) from the experimental data of Falloon and Danyushevsky (2000) are 1270 to 1350 °C, and will decrease further if an even higher water content is assumed.

The data of Umino and Kushiro (1989) and Van der Laan et al. (1989) cover the conditions proposed by Matveev and Ballhaus (2002). Their data show a slightly lower temperature range for the liquidus, from 1130 to 1260 °C.

In summary, the liquidus temperatures inferred for the trapped melt inclusions (Fig. 1 and Table 2) from our calculations (1270 to 1320 °C), the extrapolated data of Falloon and Danyushevsky (2000) (1270 to 1350 °C), and the experimental data of Umino and Kushiro (1989) and Van der Laan et al.

(1989) (1130 to 1260 °C) are very similar to those proposed by Matveev and Ballhaus (2002). The lack of olivine in the studied inclusions is a puzzling observation, because olivine will be on the liquidus under these conditions, but is not found in the trapped melt inclusions. However, in general, olivine is a relatively common type of inclusion in Os-rich PGE alloys (Capri et al. 1996). Thus, we propose that the PGE alloys formed during a process similar to that proposed by Matveev and Ballhaus (2002), but probably under slightly higher pressures and temperatures. If the boninitic melt released its water before the temperature dropped to the liquidus temperature, orthopyroxene is the solid phase on the liquidus (Table 5).

Enstatite polymorphs

Our calculations of the liquidus temperatures for the trapped melt indicate that enstatite crystallize either in the OEn structure (*Pbca* space group) or in the HTClen structure (the *C*2/*c* space group) (Fig. 4). In the latter case, the observation that the enstatite now occurs mainly in the *Pbca* ortho-enstatite structure gives some hints about the cooling history of the inclusion. Brearley and Jones (1993) showed experimentally that high temperature *C*2/*c* clino-enstatite will transform completely to ortho-enstatite if the cooling rate is smaller than a few degrees per hour. The paired clino-enstatite lamellae that occur in smaller amounts in the ortho-enstatite belong to the $P2_1/c$ structure. This feature is not surprising because neither the HP clino-enstatite nor the HT clino-enstatite structure are quenchable as the phase transformation to the LP/LTClen structure requires only slight and "energetically inexpensive" distortion of the crystal structure. The transformation to the $P2_1/c$ structure will produce antiphase domains due to a loss of a translation symmetry element. The absence of antiphase domains in the LP/LTClen lamellae indicates that the observed clino-enstatite lamellae are not a relict of an HTClen or HPClen precursor. Therefore, the most reasonable explanation for the existence of paired clino-enstatite lamellae without antiphase domains (Fig. 3) is shearing of the ortho-enstatite precursor parallel (100) (e.g., Müller 1974). This model is further supported by the observation of partial dislocations at the tip of the paired lamellae.

The stability field of LP/LT clino-enstatite provides a lower limit (>570 °C at 1 GPa; >800 °C at 7.5 GPa, Fig. 4) (Ulmer and Stalder 2001; Shimobayashi and Kitamura 1991; Arlt et al. 2000) on the ortho-enstatite crystallization temperature, which is well below our calculated crystallization temperature (Table 5). An upper limit for the temperature and pressure of formation cannot be obtained because, as discussed above, a possible HTClen or HPClen precursor phase can transform completely to ortho-enstatite without leaving any traces of its precursor.

Chromite inclusions

Our petrographic inspection of the mounted and polished iridosmine grains show that a significant fraction (~1–3%) of the studied grains contain chromite inclusions or have chromite attached to their surfaces. We observed chromite inclusions both as angular crystal fragments and as rounded to subrounded objects (Fig. 5a). The composition of the chromite inclusions fall within the range of $Fe_{0.4–0.5}Mg_{0.5–0.7}Al_{0.4–0.5}Cr_{1.5–1.7}O_4$ (see Table 5), i.e., similar to the composition to the massive chromite deposits in, e.g., the Josephine peridotite (Stockman and Hlava 1984). Selected area electron diffraction patterns were measured for several orientations of one of these chromite inclusions. They can be indexed and simulated by applying the space group as well as lattice parameters of "normal" chromite (Fig. 6). There are no indications of phase transformations, such as twinning or antiphase domains.

For the purpose of evaluating a potential high *P-T* origin of the Os-rich PGE alloys, it is useful to constrain the pressure maximum for the formation of the chromite inclusions. With

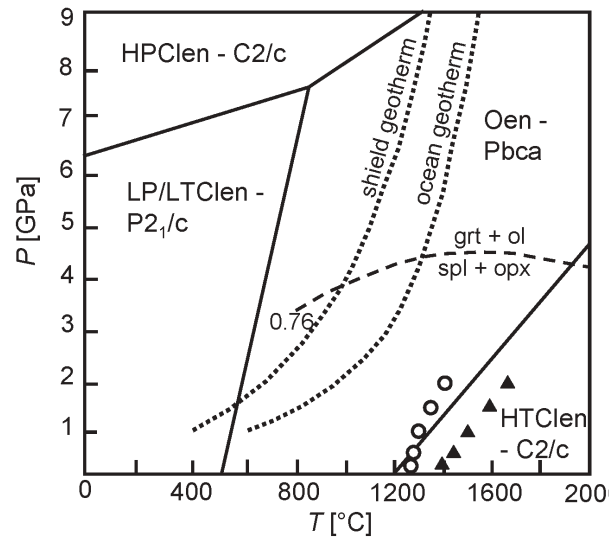

FIGURE 4. Pressure vs. temperature phase diagram of enstatite modified after Shimobayashi and Kitamura (1991), Arlt et al. (2000), and Ulmer and Stalder (2001). Phase boundaries of the enstatite polymorphs are given as bold lines. The upper stability limit of chromite with a Cr/(Cr + Al) ratio of 0.76 is indicated by a thin dashed curve. Shield geotherm and ocean geotherm after Clark and Ringwood (1964) are given as dotted lines. Additionally, the calculated liquidus temperatures (Table 4) for different pressures at dry condition (filled triangles) and 10 wt% H_2O content (open circles) are plotted. The calculated liquidus temperatures fall above the different geotherms.

TABLE 5. Calculated liquidus temperatures and crystallization of the first phase

	Dry		5% H_2O		10% H_2O	
P (GPa)	Liquidus *T* (°C)	First phase	Liquidus *T* (°C)	First phase	Liquidus *T* (°C)	First phase
Mean P1-P10						
0.2	1390	olivine	1319	olivine	1289	olivine
0.5	1437	opx	1339	olivine	1308	olivine
1.0	1518	opx	1350	opx	1335	olivine
1.5	1589	opx	1432	opx	1360	opx
2.0	1653	opx	1498	opx	1384	opx
Melt P5						
0.2	1381	opx	1320	olivine	1270	olivine
0.5	1435	opx	1331	olivine	1288	olivine
1.0	1516	opx	1378	opx	1305	olivine
1.5	1601	opx	1447	opx	1344	opx
2.0	1667	opx	1519	opx	1399	opx

Notes: The calculations were done using the program Melts (Release 1.1.0, 23 Nov. 1999) (Ghiorso and Sack 1995; Asimow and Ghiorso 1998).

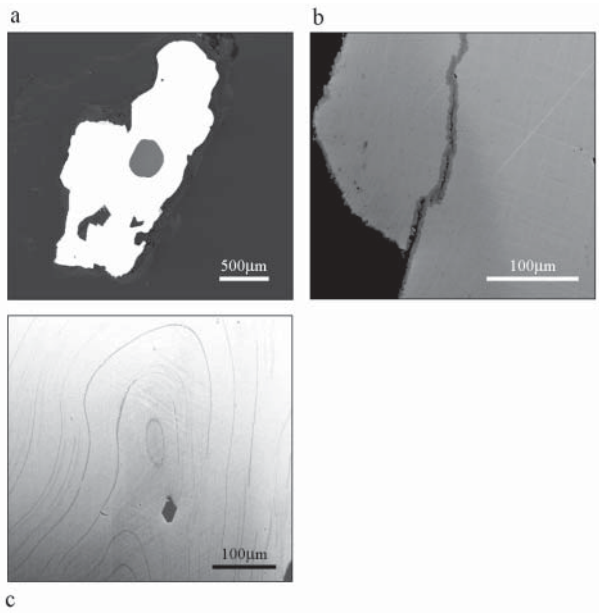

FIGURE 5. BSE images of Os-rich alloy studied in this work. (**a**) A large rounded chromite inclusion is located in the middle of the grain. (**b**) FeNi metal filling a crack in the PGE alloy; metal also can be found along the rim of the inclusion. (**c**) Growth textures in Os-rich PGE alloy. These oscillating radial textures probably indicate multiple stages of (over-) growth. A small negative crystal shape inclusion or void is located in the lower part of the image.

increasing pressure, i.e., increasing depth in the mantle, chromite reacts with enstatite to form Cr-rich garnet and olivine (Doroshev et al. 1997; Girnis and Brey 1999; Brey and Girnis 1999). However, a high Cr-content in chromite will extend its stability toward higher pressures. The upper stability limit of pure chromite is 9.5 GPa at 1000 °C and 8 GPa at 1600 °C (Doroshev et al. 1997). In the pure Fe,Mg,Al,Cr-system, the Cr/(Cr + Al) ratio of spinel in equilibrium with garnet can be used as a thermo-barometer (Girnis and Brey 1999). However, in the absence of garnet, we will only be able to estimate a maximum pressure of formation of the chromite for a specific Cr/(Cr +Al) ratio. The Cr/(Cr + Al) ratio measured in our sample range from 0.76 to 0.89 (Table 5). If we assume that all chromite grains formed in the same depth region the lowest value of 0.76 limits the pressure of formation to 4.5 GPa, well within the uppermost part of the upper mantle (Fig. 7). Depending on the exact temperature of formation, the maximum pressure of formation for chromite can be even lower.

In one rare case from the Juina area, Brazil, chromite grains were found in association with typical lower mantle and transition zone mineral phases (Kaminsky et al. 2001). In this case the unusual high amount of Ti probably stabilize chromite toward higher pressures. In contrast, the chromite grains found in the PGE alloys presented here show compositions very similar to chromites collected from the placer deposits (Table 4).

Fe-Ni metal

In some chromite inclusions, cracks are partly filled with FeNi metal. These cracks most likely formed during late-stage

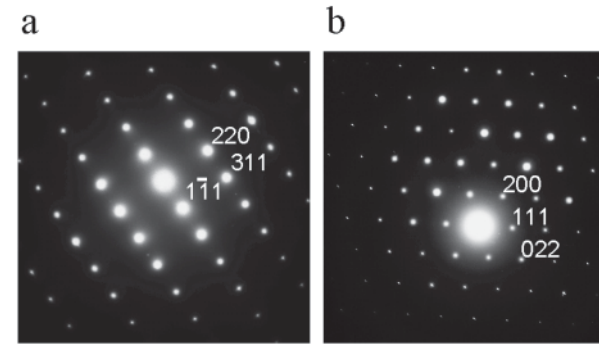

FIGURE 6. Selected area electron diffraction (SAED) pattern of chromite viewed along the $\overline{1}12$ (**a**) and $0\overline{1}1$ zone axes (**b**), respectively. The SAED patterns are consistent with the normal chromite structure.

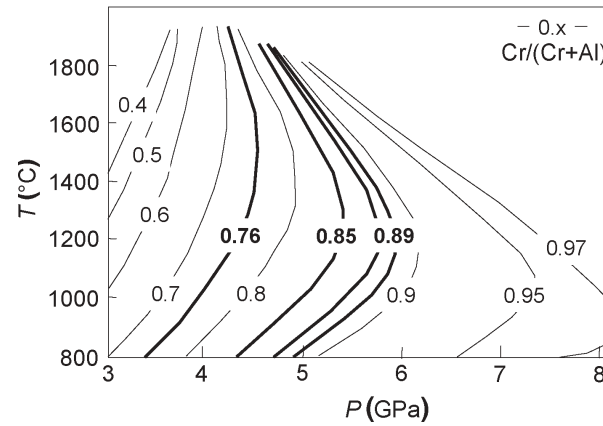

FIGURE 7. Pressure vs. temperature diagram of reaction curves of chromite + enstatite → garnet + olivine for different Cr/(Cr + Al) ratios in chromite; modified after Girnis and Brey (1999). Each reaction curve defines an upper pressure limit of the stability of Cr-rich spinel in the mantle of the earth, depending on its respective Cr/(Cr + Al) ratio. The bold lines for Cr/(Cr + Al) ratios of 0.76, 0.85, and 0.89 represent compositions of chromite found in this work.

fracturing at low pressure and clearly postdate the formation of the PGE alloys. FeNi metal forms under the reducing conditions prevailing during serpentinization of peridotite (Chamberlain et al. 1965; Dick 1974; Eckstrand 1975; Sleep et al. 2003). Such a secondary mechanism is very likely to have formed the FeNi we observe. Stockman and Hlava (1984) made similar observations of FeNi partly filling in cracks of some chromitites from the Josephine ophiolite.

DISCUSSION

If, as suggested by Bird and Bassett (1980), the Os- and Ir-rich PGE alloys were formed in the lower-most mantle or in the outer core region and were subsequently transported to the upper mantle as xenoliths in deep-rooted mantle plumes, it is to be expected that their inclusions would have mineralogic and, perhaps, also crystallographic properties consistent with a deep mantle origin. It would not be surprising if such inclusions were similar to those identified in diamonds from Sao Luiz (e.g., Harte and Harris 1994), Guinea (e.g., Stachel et al. 2000a; Brenker et al. 2002), or Juina (e.g., Kaminsky et al.

2001), which include ferroan periclase, low Ni-enstatite (former Mg-silicate perovskite), walstromite (former Ca-silicate perovskite), and majoritic garnet. However, none of these phases have been reported in Os- and Ir-rich PGE alloys, whereas typical upper mantle minerals, such as chromite, olivine, pyroxene, and laurite are frequently observed (Hagen et al. 1990; Slansky et al. 1991; Cabri et al. 1996; Malitch and Thalhammer 2002; Malitch et al. 2002; Peck et al. 1992).

Monosulfide solid solutions are believed to be the major carrier of PGEs in the upper mantle (Alard et al. 2000). During partial melting, a certain fraction (depending on the degree of partial melting) of these sulfides are dissolved in the silicate melt, which easily saturate in PGE thereby permitting the precipitation of a PGE alloy (Ballhaus 1995; Matveev and Ballhaus 2002; Brenan and Andrews 2001). Recent experimental work has established the stability limits and determined the composition of laurite, $(Ru,Os,Ir)S_2$, and RuOsIr alloys in equilibrium with mafic magmas as a function of temperature and sulfur fugacity (Brenan and Andrews 2001). Laurite and RuOsIr alloy are stable phases at chromian-spinel-based liquidus temperatures (i.e., $T < 1300$ °C) in the absence of an immiscible sulfide liquid. These results provide confirmation of the view that Os-rich PGE alloys can form as early cumulates during crystallization of primitive magmas under typical upper mantle or lower crustal magmatic conditions (e.g., Talkington et al. 1984; Peck et al. 1990, 1992; Cabri et al. 1996; Matveev and Ballhaus 2002).

The intimate association of the Os-rich PGE alloys with chromite, both as host phase and as inclusion, strongly suggests that the formation of these alloys must be understood within a model that also explains the precipitation of massive chromite deposits and the remarkable nodular textures, which characterize many undeformed chromite deposits. Recently, Ballhaus (1998) and Matveev and Ballhaus (2002) have conducted a set of innovative experiments in which they were able to achieve rapid and effective concentration of chromite and, at the same time, account for the nodular textures that are observed in natural settings. These experiments were conducted at temperatures from 1200 to 1150 °C and pressures from 1 atm to 0.4 GPa, and took advantage of slow mixing or immiscibility between basalts of different composition and between basalt and hydrous fluids.

In the second set of experiments (Matveev and Ballhaus 2002), strong immiscibility was achieved between an olivine-chromite normative melt and a hydrous fluid. Upon olivine and chromite precipitation, chromite would collect in the hydrous liquid droplets, while olivine collected in the basaltic melt. This fractionation is driven by different interfacial energies between chromite and hydrous fluid and basaltic melt, respectively. These findings suggest that exolution of a hydrous fluid from an olivine-chromite saturated melt will result in a strong concentration of chromite in the hydrous fluid. Subsequent settling and annealing of such chromite-rich droplets cause the formation of chromite deposits with nodular textures. Matveev and Ballhaus (2002) furthermore demonstrated that precipitated PGE-rich metallic alloys will concentrate with the chromite in the hydrous fluid phase.

The experiments described above (Brenan and Andrews 2001; Ballhaus 1998; Matveev and Ballhaus 2002) are relevant to the conditions encountered in an arc environment. In a supra-subduction setting, dehydration of the downgoing slab will release immiscible hydrous fluids and form boninitic melts in the overlying mantle. Thus, the proposed mechanism for chromite concentration (Matveev and Ballhaus 2002) can be at work in an arc environment in the presence of hydrous fluids where simultaneous precipitation of Os-rich PGE alloys and laurite, olivine, and chromite, and the concentration of chromite, PGE alloy, and laurite in immiscible hydrous liquids is possible. This model can explain all key observations, including (1) the formation of massive chromite deposits; (2) nodular chromite textures; (3) Os-rich PGE alloys, laurite, olivine, and pyroxene as fairly common inclusions in chromite (Stockman and Hlava 1984, Talkington et al. 1984; Bai et al. 2000; Melcher et al. 1997), and (4) inclusions of chromite, olivine, pyroxene (Hagen et al. 1990; Slansky et al. 1991; Cabri et al. 1996; Malitch and Thalhammer 2002; Malitch et al. 2002; Peck et al. 1992), and hydrated siliceous melt inclusions (the present study) in the Os-rich PGE alloys.

Os isotopic compositions of Os-rich PGE alloys and chromitites

Bird et al. (1999) reported radiogenic $^{186}Os/^{188}Os$ ratios in two Os-rich PGE alloys from Port Orford, similar to those studied here. The excesses of radiogenic ^{186}Os measured in these two alloys were similar to those measured previously in Hawaiian and Siberian basalts by Brandon et al. (1998). Brandon et al. (1998) argued that coupled enrichment in $^{186}Os/^{188}Os$ and $^{187}Os/^{188}Os$ in the Hawaiian and Siberian basalts is a signature of the present day outer core. In this model, the outer core was proposed to have evolved to radiogenic Os isotopic compositions as a result of inner core formation that led to fractionated (i.e., higher than chondritic) Re/Os and Pt/Os elemental ratios in the outer core. Within the context of the Brandon et al. model, Bird et al. (1999) used their data to argue in favor of an outer-core origin of the Os-rich PGE alloys, as originally proposed by Bird and Bassett (1980).

Meibom and Frei (2002) presented $^{186}Os/^{188}Os$ and $^{187}Os/^{188}Os$ ratios on a larger set of Os-rich PGE alloys from northern California and southwest Oregon. This larger data set demonstrated that an outer-core origin of the radiogenic Os in the Os-rich PGE alloys requires that the inner core grew to its present size extremely early in the evolution of the Earth; within several hundred million years after accretion. This is not a realistic constraint, because such early core formation would result in a much larger size for the present day inner core, even if the assumed heat flux across the core-mantle boundary is taken to be its estimated present day minimum (i.e., 3 TW) (Labrosse et al. 2001). Geophysical modeling suggests that, even with the minimum heat flux across the core-mantle boundary, the inner core could not have started to form earlier than about 2.5–3 Ga, and would have continued to grow until the present day.

As an alternative to an outer-core origin, it was suggested that radiogenic Os isotopic compositions similar to those measured in the Hawaiian and Siberian basalts could result from common upper mantle processes. Smith (2003) has argued that "wet-spot" compositions formed by fluid metasomatism, e.g.,

at convergent margins, can produce a range of radiogenic $^{186}Os/^{188}Os$ and $^{187}Os/^{188}Os$ ratios, similar to those measured in the Hawaiian and Siberian basalts (Brandon et al. 1998) and in the Os-rich PGE alloys (Bird et al. 1999; Meibom and Frei 2002), on a time scale of about 2 Gy. Alternatively, the observed range of $^{186}Os/^{188}Os$ and $^{187}Os/^{188}Os$ ratios in these samples could be generated from depleted upper mantle lithologies on a shorter time scale (150–200 My) by partitioning of PGEs into pyroxenites precipitated from Mg-rich melts (Smith 2003; Meibom et al. in preparation). Both of these scenarios provide a realistic alternative to the outer core as the source of the radiogenic Os in the Os-rich PGE alloys and are broadly consistent with the constraints presented above in terms of the chemistry of the silicate and chromite inclusions.

Finally, Meibom et al. (2002) reported $^{187}Os/^{188}Os$ ratios for more than 700 Os-rich PGE alloys from northern California and southwest Oregon. This data set forms a broad, essentially Gaussian distribution centered around a $^{187}Os/^{188}Os$ ratio of about 0.1245 (a typical upper mantle value) and span 6–7 γ_{Os} units (calculated relative to the average $^{187}Os/^{188}Os$ ratio of 0.1245). The Gaussian shape of the $^{187}Os/^{188}Os$ distribution is, in all likelihood, a signature of random mixing processes between depleted (unradiogenic) and enriched (radiogenic) domains during partial melting in the upper mantle (Meibom et al. 2002). A similar variation in $^{187}Os/^{188}Os$ was reported by Hattori and Hart (1991) among Os-rich PGE alloys and laurite samples derived from individual ultramafic rocks around the world. Importantly, recent Os isotopic analyses of chromite from various peridotite bodies around the world (Walker et al. 2002) showed similar variation in $^{187}Os/^{188}Os$ among chromites from a single locality. This finding is consistent with the general formation model discussed above, in which chromite and Os-rich PGE alloys form in the same process with Os supplied from a very heterogeneous upper mantle by partial-melting events. Although we have not, at this point, systematically measured $^{187}Os/^{188}Os$ on chromites derived from the peridotite bodies in northern California and southwest Oregon, we predict that they will show similar $^{187}Os/^{188}Os$ variation and, provided the number of chromite analyses become large enough, will form a Gaussian distribution similar to that observed for the Os-rich PGE alloys (Meibom et al. 2002). We also predict that occasional enrichments in $^{186}Os/^{188}Os$, similar to those measured in Os-rich PGE alloys, will be found in these chromite samples.

ACKNOWLEDGMENTS

We are grateful to W.F. Müller (Darmstadt), T. Walther, and W. Mader (Bonn) for access to TEM facilities for this project. Inspiring discussions with Robert Coleman and Chris Ballhaus are greatly appreciated.

REFERENCES CITED

Alard, O., Griffin, W. L., Lorand, J. P., Jackson, S. E., and O'Reilly, S. Y. (2000) Non-chondritic distribution of the highly siderophile elements in the sulfides. Nature, 407, 891–894.

Amossé, J., Dablé, P., and Allibert, M. (2000) Thermochemical behaviour of Pt, Ir, Rh and Ru vs. f_{O_2} and f_{S_2} in a basaltic melt. Implications for the differentiation and precipitation of these elements, Mineralogy and Petrology, 68, 29–62.

Arlt, T., Kunz, M., Stolz, J., Armbruster, T., and Angel, R.J. (2000) *P-T-X* data on $P2_1/c$-clinopyroxenes and their displacive phase transitions. Contributions to Mineralogy and Petrology, 138, 35–45.

Asimow, P.D. and Ghiorso, M.S. (1998) Algorithmic Modifications Extending MELTS to Calculate Subsolidus Phase Relations. American Mineralogist, 83, 1127–1131.

Auge, T. and Johan, Z. (1988) Comparative study of chromite deposits from Troodos, Vourinos, North Oman and New Caledonia ophiolites. In J. Boissonnas and P. Omenetto, Eds., Mineral Deposits in the European Community, p. 267–288, Springer-Verlag, Heidelberg.

Bai, W., Robinson, P.T., Fang, Q., Yang, J., Yan, B., Zhang, Z., Hu, X.-F., Zhou, M.-F., and Malpas, J. (2000) The PGE and base-metal alloys in the podiform chromitites of the Luobusa ophiolite, Southern Tibet, Canadian Mineralogist, 38, 585–598.

Ballhaus, C. (1995) Is the upper mantle metal-saturated? Earth and Planetary Science Letters, 132, 75–86.

——— (1998) Origin of podiform chromite deposits by magma mingling. Earth and Planetary Science Letters, 156, 185–193.

Barnes, S.-J., Naldrett, A.J., and Gorton, M.P. (1985) The origin of the fractionation of platinum-group elements in terrestrial magmas. Chemical Geology, 53, 303–323.

Bird, J.M. and Bassett, W.A. (1980) Evidence of a Deep Mantle History in Terrestrial Osmium-Iridium-Ruthenium Alloys. Journal of Geophysical Research, 85 (B10), 5461–5470.

Bird, J.M. and Weathers, M.S. (1975) Josephinite: specimens from the Earth's core? Earth and Planetary Science Letters, 28, 51–64.

——— (1979) Origin of josephinite. Geochemical Journal, 13, 41–55.

Bird, J.M., Bassett, W., and Weathers, M.S. (1979) Widmanstätten patterns in josephinite, a metal bearing terrestrial rock. Science, 206, 832–834.

Bird, J.M., Meibom, A., Frei, R., and Naegler, T.F. (1999) Osmium and lead isotopes of rare OsIrRu minerals: derivation from the core-mantle boundary region? Earth and Planetary Science Letters, 170, 83–92.

Brandon, A.D., Norman, M.D., Walker, R.J., and Morgan, J.W. (1999) ^{186}Os-^{187}Os systematics of Hawaiian picrites. Earth and Planetary Science Letters, 174, 25–42.

Brearley A.J. and Jones, R.H. (1993) Chondrite thermal histories from low-Ca pyroxene microstructures: autometamorphism vs. prograde metamorphism revisited. Lunar and Planetary Science Conference XXIV, 185–186.

Brenan, J.M. and Andrews, D. (2001) High-temperature stability of laurite and Ru-Os-Ir alloy and their role in PGE fractionation in mafic magmas. Canadian Mineralogist, 39, 341–360.

Brenker, F.E., Stachel, T., and Harris, J.W. (2002) Exhumation of lower mantle inclusions in diamond—ATEM investigation of retrograde phase transitions, reactions and exsolution. Earth and Planetary Science Letters, 198, 1–9.

Brey, G.P. and Girnis, A.V. (1999) Garnet-spinel-olivine-orthopyroxene equilibria in the FeO-MgO-Al_2O_3-SiO_2-Cr_2O_3 system: I. Composition and molar volumes of minerals. European Journal of Mineralogy, 11, 599–617.

Cabri, L.J., Harris, D.C., and Weiser, T.W. (1996) Mineralogy and Distribution of Platinum-group Mineral (PGM) Placer Deposits of the World. Exploration and Mining Geology, 5, 73–167.

Chamberlain, J.A. (1965) Native metals in the Muskov intrusion. Canadian Journal of Earth Sciences, 2, 188–215.

Coleman, R.G. (2000) Prospecting for ophiolites along the California continental margin. In Y. Dilek, E. Moores, D. Elthon, and A. Nicolas, Eds., Ophiolites and Oceanic Crust, p. 351–364, Geological Society of America Special Paper, Boulder.

Collerson, K.D. Hapugoda, S., Kamber, B.S., and Williams, Q. (2000) Rocks from the mantle transition zone: Majorite-bearing xenoliths from Malaita, southwest Pacific. Science, 288, 1215–1223.

Dick, H.J.B. (1974) Terrestrial nickel-iron from the Josephine peridotite, its geological occurrence, associations, and origin. Earth and Planetary Science Letters, 24, 291–298.

Dick, H.J.B. and Gillete, H. (1976) Josephinite—specimens from the core? A discussion. Earth and Planetary Science Letters, 31, 308–311.

Doroshev, A.M., Brey, G.P., Girnis, A.V., Turkin A.I., and Kogarko, L.N. (1997) Pyrope-knorringite garnets in the earths mantle: Experiments in the MgO-Al_2O_3-SiO_2-Cr_2O_3 system. Geologiya I Geofizika, 38, 523–545.

Eckstrand, O.R. (1975) The Dumont serpentinite: a model for control of nickeliferous opaque mineral assemblages by alteration reactions in ultramafic rocks. Economic Geology and the Bulletin of the Society of Economic Geologist, 70, 183–201.

Falloon, T.J. and Danyushevsky, L.V. (2000) Melting of refractory mantle at 1.5, 2 and 2.5 Gpa under anhydrous and H2O-undersaturated conditions: Implications for the petrogenesis of high-Ca boninites and the influence of subduction components on mantle melting. Journal of Petrology, 41, 257–283.

Fleet, M.E. and Stone, W.E. (1991) Partitioning of Platinum-group elements in the Fe-Ni-S system and their fractionation in nature. Geochimica et Cosmochimica Acta, 55, 245–253.

Ghiorso, M.S. and Sack, R.O. (1995) Chemical mass transfer in magmatic processes. IV. A revised and internally consistent thermodynamic model for the interpolation and extrapolation of liquid-solid equilibria in magmatic systems at elevated temperatures and pressures. Contributions to Mineralogy and Petrology, 119, 197–212.

Girnis, A.V. and Brey, G.P. (1999) Garnet-spinel-olivine-orthopyroxene equilibria in the FeO-MgO-Al_2O_3-SiO_2-Cr_2O_3 system: II. Thermodynamic analysis. European Journal of Mineralogy, 11, 619–636.

Hagen, D., Weiser, T., and Htay, T. (1990) Platinum-Group Minerals in Quaternary Gold Placers in the Upper Chindwin Area of Northern Burma. Mineralogy and Petrology, 42, 265–286.

Harper, G.D. (1984) The Josephine ophiolite, northwestern California. Geological Society of America Bulletin, 95, 1009–1026.

Harper, G.D., Grady, K., and Wakabayashi, J. (1990) A structural study of a metamorphic sole beneath the Josephine ophiolite, western Klamath terrane, California-Oregon. Geological Society of America, Special paper 255, 379–396.

Harris, D.C. and Cabri, L.J. (1973) The nomenclature of natural alloys of osmium, iridium and ruthenium based on new compositional data of alloys from worldwide occurrences. Canadian Mineralogist, 12, 104–112.

——— (1991) Nomenclature of platinum-group-element alloys: Review and revision. Canadian Mineralogist, 29, 231–237.

Harte, B. and Harris, J.W. (1994) Lower mantle associations preserved in diamonds. Mineralogical Magazine, 58A, 384–385.

Hattori, K. and S.R. Hart (1991) Osmium-isotope ratios of platinum-group minerals associated with ultramafic intrusions: Os-isotope evolution of the oceanic mantle, Earth and Planetary Science Letters, 107, 499–514.

Johan, Z., Ohnenstetter, M., Fischer, W., and Amosse, J. (1990) Platinum-Group Minerals from the Durance River Alluvium, France. Mineralogy and Petrology, 42, 287–306.

Kaminsky, F.V., Zakharchenko, O.D., Davies, R.,Griffin, W.L., Khachatryan-Blinova, G.K., and Shiryaev, A.A. (2001) Superdeep diamonds from the Juina area, Mato Grosso State, Brazil. Contributions to Mineralogy and Petrology, 140, 734–753.

Labrosse, S., Poirier, J.-P., and Mouel, J.-L.L. (2001) The age of the inner core. Earth and Planetary Science Letters, 190, 111–123.

Leblanc, M. (1991) Platinum-Group Elements and Gold in Ophiolitic Complexes: Distribution and Fractionation from Mantle to Oceanic Floor. In T.P., Ed., Ophiolite Genesis and Evolution of the Oceanic Lithosphere, p. 231–260, Ministry of Petroleum and Minerals, Sultanate of Oman.

Malitch, K.N. and Thalhammer, O.A.R (2002) Pt-Fe nuggets derived from clinopyroxenite-dunite massifs, Russia: A structural, compositional and osmium isotope study. Canadian Mineralogist, 40, 395–418.

Malitch, K.N., Auge, T., Badanina, I.Y., Goncharov, M.M., Junk, S.A., and Pernicka, E. (2002) Os-rich nuggest from Au-PGE placers of the Maimecha-Kotui Province, Russia: a multi-disciplinary study. Mineralogy and Petrology, 76, 121–148.

Matveev, S. and Ballhaus, C. (2002) Role of water in the origin of podiform chromitite deposits. Earth and Planetary Science Letters, 203, 235–243.

McElduff, B. and Stumpfl, E.F. (1990) Platinum-Group Minerals from the Troodos Ophiolite, Cyprus. Mineralogy and Petrology, 42, 211–232.

Meibom, A. and Frei, R. (2002) Evidence for an Ancient Osmium Isotopic Reservoir in Earth. Science, 296, 516–518.

Meibom, A., Sleep, N.H., Chamberlain, C.P., Coleman, R.G., Frei, R., Hren, M.T., and Wooden, J.L. (2002) Re-Os isotopic evidence for long-lived heterogeneity and equilibrium processes in Earth's upper mantle. Nature, 419, 705–708.

Melcher, F., Grum, W., Simon, G., Thalhammer, T.V., and Stumpfl, E.F. (1997) Petrogenesis of the Phiolitic Giant Chromite Deposit of Kempirsai, Kazakstan: a Study of Solid and Fluid Inclusions in Chromite, Journal of Petrology, 38, 1419–1458.

Müller, W.F. (1974) One-dimensional lattice imaging of a deformation-induced lamellar intergrowth of orthoenstatite and clinoenstatite $(Mg,Fe)SiO_3$. Neues Jahrbuch für Mineralogie Monatshefte, 1974, 83–88.

Nakagawa, M. and Franco, H.E.A. (1997) Placer Os-Ir-Ru alloys and sulfides: Indicators of sulfur fugacity in an ophiolite? Canadian Mineralogist, 35, 1441–1452.

Nilsson, L.P. (1990) Platinum-Group Mineral Inclusions in Chromite from the Osthammeren Ultramafic Tectonite Body, South Central Norway. Mineralogy and Petrology, 42, 249–263.

Peck, D.C. and Keays, R.R. (1990) Insights into the behavior of precious metals in primitive, S-undersaturated magmas: Evidence from the Heazelwood River Complex, Tasmania. Canadian Mineralogist, 28, 553–577.

Peck, D.C., Keays, R.R., and Ford, R.J. (1992) Direct crystallization of refractory platinum group element alloys from boninitic magmas: evidence from western Tasmania. Australian Journal of Earth Science, 39, 373–387.

Ramp, L. (1961) Chromite in southwestern Oregon, p. 169. Department of Geology and Mineral Industries, State of Oregon.

Rehkämper, M., Halliday, A.N., Fitton, J.G., Lee, D.-C., Wieneke, M., and Arndt, N.T. (1999) Ir, Ru, Pt, and Pd in basalts and komatiites: New constraints for the geochemical behaviour of the platinum-group elements in the mantle. Geochimica et Cosmochimica Acta, 63, 3915–3934.

Shimobayashi, N. and Kitamura, M. (1991) Phase transition in Ca-poor clinopyroxenes. Physics and Chemistry of Minerals, 18, 153–160.

Slansky, E., Johan, Z., Ohnenstetter, M., Barron, L.M., and Suppel, D. (1991) Platinum mineralization in the Alaskan-type instrusive complexes near Fifield, N. S. W., Australia. Part 2. Platinum-Group minerals in placer deposits at Fifield. Mineralogy and Petrology, 43, 161–180.

Sleep, N.H., Meibom A., Fridriksson Th., Bird D. K., and Coleman R. G. (2003) H_2-rich fluids from serpentinization: Geochemical and biotic implications. Proceedings of the National Academy of Sciences, in press.

Smith, A.D. (2003) Critical evaluation of Re-Os and Pt-Os isotopic evidence on the origin of intra plate volcanism. Journal of Geodynamics, in press.

Sobolev, A.V. and Chaussidon, M. (1996) H_2O concentrations in primary melts from supra subduction zones and mid-ocean ridges: Implications for H_2O storage and recycling in the mantle. Earth and Planetary Science Letters, 137, 45–55.

Stachel, T., Brey, G.P., and Harris, J.W. (2000) Kankan diamonds (Guinea) I: from the lithosphere down to the transition zone. Contributions to Mineralogy and Petrology, 140, 1–15.

Stachel, T., Harris, J.W., Brey, G.P., and Joswig, W. (2000) Kankan diamonds (Guinea) II: lower mantle inclusion parageneses. Contributions to Mineralogy and Petrology, 140, 16–27.

Stockman, H. and Hlava, P.F. (1984) Platinum-Group Minerals in Alpine Chromitites from Southwestern Oregon. Economic Geology, 79, 491–508.

Talkington, R.W., Watkinson, D.H., Whittaker, P.J., and Jones, P.C. (1984) Platinum-group minerals and other solid inclusions in chromite of ophiolitic complexes: occurence and petrological. Tschermaks Mineralogische und Petrographische Mitteilungen, 32, 285–301.

Tornroos, R. and Vuorelainen, Y. (1987) Platinum-group metals and their alloys in nuggets from alluvial deposits in Finnish Lapland. Lithos, 29, 491–500.

Ulmer, P. and Stalder, R. (2001) The $Mg(Fe)SiO_3$ othoenstatite-clinoenstatite transitions at high pressures and temperatures determined by Raman-spectroscopy on quenched samples. American Mineralogist, 86, 1267–1274.

Umino, S. and Kushiro, I. (1989) Experimental studies on boninite petrogenesis. In Crawford, A.J., Ed., Boninites and related Rocks, 89–111. Unwyn and Hyman, London.

Van Capellen, E. and Doukhan, J.C. (1994) Quantitative transmission X-ray microanalysis of ionic compounds. Ultramicroscopy, 53, 343–349.

Van der Laan, S.R., Flower, M.F.J., and Koster von Groos, A.F. (1989) Experimental evidence for the origin of boninites: near-liquidus phase relations to 7.5 kbar. In Crawford, A.J., Ed., Boninites and related Rocks, 112–147. Unwyn and Hyman, London.

Walker, R.J. and Nisbet, E. (2002) Os^{187} isotopic constraints on Archean mantle dynamics. Geochimica et Cosmochimica Acta, 66, 3317–3325.

Walker, R.J., Morgan, J.W., Beary, E.S., Smoliar, M.I., Czamanske, G.K., and Horan, M.F. (1997) Applications of the ^{190}Pt-^{186}Os isotope system to geochemistry and cosmochemistry. Geochimica et Cosmochimica Acta, 61, 4799–4807.

MANUSCRIPT RECEIVED NOVEMBER 6, 2002
MANUSCRIPT ACCEPTED JULY 11, 2003
MANUSCRIPT HANDLED BY GRAY BEBOUT